Acta Cryst. (1966). **20**, 572

AB Compounds with Sc, Y and Rare Earth Metals. II. FeB and CrB Type Structures of Monosilicides and Germanides*

By D. Hohnke and E. Parthé

Metallurgy Department and Laboratory for Research on the Structure of Matter, University of Pennsylvania, Philadelphia, Pa., U.S.A.

(*Received* 30 *July* 1965)

Twenty new rare earth silicides and germanides of composition *AB* have been synthesized and their crystal structures have been determined. LaSi, CeSi, PrSi, NdSi, SmSi, GdSi, TbSi, DySi, HoSi, ErSi, LaGe, CeGe, PrGe crystallize in the FeB (*B*27) structure type. DySi, HoSi, ErSi, PrGe, NdGe, SmGe, GdGe, TbGe, DyGe, HoGe and ErGe crystallize in the CrB structure type. Polymorphism occurs in DySi, HoSi, ErSi and PrGe which crystallize in both of these structure types.

The FeB- and CrB-type structures contain a common structural unit, the trigonal prism, which is stacked differently to form either structure. On this basis, a set of transformation equations relating the lattice constants of both structure types is derived.

A survey of all known FeB- and CrB-type structures shows that these compounds occur only in two valence electron concentration ranges. The shape of the prism side within each range depends on the valence electron difference.

Introduction

In two earlier communications it was reported that the scandium and yttrium monogermanides and monosilicides crystallize with the CrB structure type, which is also known as the TlI (*B*33) type. (Parthé, 1959; Schob & Parthé, 1965). It was of interest here to investigate if the monosilicides and monogermanides of the rare earths exist and if they form the same structure type. Owing to the similar outer electron configuration the structures observed for scandium and yttrium compounds are often similar to those for the corresponding lanthanide compounds. However, exceptions to this general behavior are known. For example, the $ZrSi_2$ (*C*49) structure type observed for $ScGe_2$ (Schob & Parthé, 1964) does not occur for other rare earth digermanides. The anomaly of $ScGe_2$ can perhaps be explained by the comparatively small size of the scandium atom. The variety of structure types for the other rare earth digermanides which may crystallize with the related AlB_{2-x}, $EuGe_2$, $ThSi_2$ or $GdSi_2$ structure types is unexpected and can not be explained by size differences. Thus, although the outer electron configuration of the lanthanide elements from La to Lu is either $5d^16s^2$ or $5d^06s^2$, their alloying behavior with a particular alloying partner can show surprising differences from one rare earth element to the next. Unfortunately the elementary principles of the alloy formation for rare earth alloys are not really understood. The study of these structural differences may provide some clues on how to attack the problem.

Experimental

Rare earth elements used in this investigation were provided by Nuclear Corporation, Research Chemicals Division, Phoenix and had a stated purity of 99·9%. Samples of LaSi, CeSi, PrSi, NdSi, SmSi, GdSi, TbSi, DySi, HoSi, ErSi and LaGe, CeGe, PrGe, NdGe, GdGe, TbGe, HoGe and ErGe were prepared by direct synthesis from the elements under an argon atmosphere in an arc-furnace. To improve homogeneity of the reaction product the arc-melted buttons were turned at least three times and remelted. Weighing the specimens after reaction to check the composition showed negligible loss of substance.

SmGe was prepared by sintering a compacted pellet of the mixed powders in an evacuated quartz tube at 400 °C, then gradually raising the temperature to 800 °C in four days.

Lattice constants of the different compounds were obtained from powder X-ray diffraction patterns prepared with filtered Cu $K\alpha_1$ ($\lambda = 1{\cdot}5405$ Å) or Cr $K\alpha_1$ ($\lambda = 2{\cdot}2896$ Å) radiation by minimizing the difference between calculated and observed $\sin^2\theta$ values for the last 15 lines.

Results of structure investigation

Compounds with FeB (*B*27) structure type

A number of the investigated compounds were found to crystallize with the FeB (*B*27) structure type. A complete intensity calculation was performed on LaSi.

The powder X-ray diffractometer pattern of LaSi showed the lines of an orthorhombic unit cell with the lattice constants $a = 8{\cdot}404 \pm 0{\cdot}005$, $b = 4{\cdot}010 \pm 0{\cdot}003$ and $c = 6{\cdot}059 \pm 0{\cdot}003$ Å. Systematic extinctions were observed for $hk0$ with $h = 2n+1$ and for $0kl$ with $k+l = 2n+1$, which lead to the following possible space groups: $Pn2_1a$ (C_{2v}^9) and $Pnma$ (D_{2h}^{16}). The great similarity of the LaSi pattern with a diffraction pattern of ZrSi (FeB (*B*27) structure type) and the agreement in the extinction laws suggested structural analogy with the latter. On this basis a trial intensity calculation was

* Part I: O. Schob & E. Parthé (1965). *Acta Cryst.* **19**, 214.

performed with a computer program designed in this laboratory* and assuming space group *Pnma* (D_{2h}^{16}) with point positions 4(*c*) for La and 4(*c*) for Si. The initial positional parameters were that of ZrSi (Schachner, Nowotny & Kudielka, 1954). Variation of positional parameters in steps of 0·001 and consideration of an overall isotropic temperature factor $B=1{\cdot}4\times 10^{-16}$ cm^2 obtained with a procedure given by Buerger (1960) lead to the following refined parameter values:

4La in 4(*c*) $x_A=0{\cdot}178\pm0{\cdot}001$

$z_A=0{\cdot}119\pm0{\cdot}001$

4Si in 4(*c*) $x_B=0{\cdot}032\pm0{\cdot}01$

$z_B=0{\cdot}611\pm0{\cdot}01$

It was observed that the Si positional parameters were not very sensitive to small variations. The positional parameter values for Si in ZrSi also gave the best results in LaSi. The agreement between the observed ${}^0F_o$ values (obtained from area of diffractometer peaks integrated with planimeter) and calculated values is good, as seen in Table 1. The residual $R=\Sigma||{}^0F_o|-|{}^0F_c||/\Sigma|{}^0F_o|$ for 77 observed and unobserved reflections was 0·094.

* The atomic scattering factors used in this calculation were obtained from analytical expressions given by Moore (1963).

Table 1. *Intensity calculation for* LaSi *with* FeB (*B*27) *structure type*

Cu $K\alpha$-radiation

hkl	d_c	$10^3\sin^2\theta_c$	$10^3\sin^2\theta_o$	I_o	${}^0F_o$	${}^0F_c$
101	4·911 Å	24·6	24·5	12	15·0	14·2
200	4·200	33·6	33·4	30	40·0	−40·9
201	3·452	49·8	49·5	48	43·6	−48·4
011	3·343	53·1	52·9	68	53·3	−53·5
111	3·110	61·5	61·4	160	64·0	−62·7
002	3·024	64·8	—	<1	14·8*	11·7
210	2·901	70·5	70·3	135	89·7	−87·5
102	2·846	73·2	73·2	196	108·3	−93·5
211	2·615	86·7	86·4	74	83·3	84·4
301	2·541	91·8	91·8	72	76·3	−83·9
202	2·456	98·4	—	<1	5·7*	−0·9
112	2·322	110·1	109·9	90	67·4	−63·2
311	2·146	128·7	128·2	9	23·5	23·8
400	2·100	134·4	—	<1	9·9*	7·5
212	2·092	135·3	—	<1	4·8*	−7·0
302	2·056	140·4	—	<1	7·3*	8·0
020	2·004	147·6	147·6	57	123·6	−113·0
401	1·985	150·6	149·8	33	70·0	70·3
103	1·959	154·2	154·1	2	17·4	−14·9
410	1·859	171·3	170·4	24	64·7	73·3
121	1·855	172·2	172·1	4	18·6	−13·8
312	1·827	177·3	176·9	60	74·9	71·5
203	1·818	179·4	179·1	19	59·6	−48·5
220	1·808	181·2	180·8	12	47·2	36·5
013	1·801	182·7	182·6	22	65·2	−52·8
411	1·778	187·5	187·3	2	12·1	23·1
113	1·762	191·1	190·7	23	48·0	47·9
221	1·732	197·4	197·2	12	35·9	42·4
402	1·724	199·2	—	<1	9·2*	0·8
022	1·671	212·4	—	<1	9·5*	−10·0
213	1·655	216·3	216·1	33	63·2	57·7
122	1·639	220·8	220·7	68	†	82·0
303	1·636	221·4			†	60·9
501	1·619	226·2	225·3	8	46·3	41·2
412	1·585	236·1	—	<1	7·3*	3·9

Table 1 (*cont.*)

hkl	d_c	$10^3\sin^2\theta_c$	$10^3\sin^2\theta_o$	I_o	${}^0F_o$	${}^0F_c$
321	1·574	239·4	238·9	30	64·7	73·9
222	1·553	246·0	—	<1	7·5*	1·0
313	1·515	258·3	259·0	26	†	−16·5
004	1·513	259·2			†	−101·7
511	1·501	263·1	262·2	17	50·7	51·8
104	1·488	267·6	—	<1	11·1*	−12·7
502	1·467	274·8	274·2	3	31·5	38·3
403	1·454	280·2	279·6	13	66·4	75·4
420	1·450	282·0	—	<1	11·6*	7·1
322	1·434	288·0	—	<1	8·2*	−7·6
204	1·424	292·4	292·7	4	35·4	35·3
421	1·410	298·2	297·3	14	50·9	−63·5
123	1·402	301·8	300·5	2	19·4	13·9
600	1·401	302·4	302·2	8	77·8	82·1
114	1·396	304·5	—	<1	8·7*	−11·5
512	1·380	311·7	310·6	20	62·5	−72·9
413	1·368	317·1	316·9	3	22·5	26·1
601	1·364	318·6	—	<1	12·6*	−12·4
223	1·347	327·0	327·0	7	38·8	44·4
214	1·341	329·7	329·6	25	72·7	70·1
304	1·331	334·8	—	<1	13·1*	−0·9
610	1·322	339·3	338·5	6	49·0	−50·3
422	1·308	346·8	—	<1	9·4*	−0·7
031	1·305	348·3	348·8	4	40·0	43·9
611	1·292	355·5	356·8	14·5	†	−46·0
503	1·291	355·8			†	−34·1
131	1·290	356·7			†	50·6
230	1·273	365·7	366·0	9	64·5	70·0
602	1·271	367·2	—	<1	13·8*	6·6
323	1·267	369·0	368·8	11	52·1	−56·1
314	1·263	371·7	—	<1	10·4*	6·8
521	1·259	373·8	373·8	5	30·6	−38·2
231	1·246	381·9	381·9	7	42·4	−43·7
513	1·229	392·6	392·1	3	30·8	−38·8
404	1·228	393·6	—	<1	14·5*	7·4
612	1·211	404·1	—	<1	10·2*	−5·2
132	1·210	405·3	405·5	8	47·0	50·7
024	1·207	406·8	406·8	15	85·3	93·9
105	1·198	413·4	—	<1	14·8*	−12·8
124	1·195	415·2	—	<1	10·9*	11·8
522	1·185	422·4	421·9	4	31·8	−35·7
331	1·183	423·9	—	<1	10·7*	−19·4

* One half of the F value obtained from the smallest observable intensity value.

† Separate ${}^0F_o$ values for superimposed diffraction lines cannot be determined.

The same FeB structure type was also found for twelve other compounds: CeSi, PrSi, NdSi, SmSi, GdSi, TbSi, DySi, HoSi, ErSi, LaGe, CeGe and PrGe. Their lattice constants are given in Table 2. With the exception of HoSi (see Table 3), no intensity calculations were performed for these compounds; however, the intensities of the observed lines correspond to those of LaSi if the differences of atomic scattering are considered. Some of the listed compounds have a second modification with the CrB structure type which will be discussed below.

While this paper was being prepared for publication we received notice of recent studies on rare earth monosilicides by Gladyshevskii & Kripyakevich (1964) and on monogermanides by Tharp, Smith & Johnson (1966). Their results have been added to Tables 2 and 4; they are essentially identical with those reported here.

Table 2. *AB compounds with* FeB (*B*27) *structure type*

	Lattice parameters for setting *Pnma*			Adjustable parameters ($r_A > r_B$)				Ref.
	a(Å)	b(Å)	c(Å)	x_A	z_A	x_B	z_B	
Group I compounds								
LaSi	8·404 ± 0·005	4·010 ± 0·003	6·059 ± 0·003	0·178 ± 0·001	0·119 ± 0·001	0·032 ± 0·01	0·611 ± 0·01	(1)
	8·48 ± 0·02	4·02 ± 0·01	6·04 ± 0·01					(25)
LaGe	8·486 ± 0·005	4·134 ± 0·003	6·119 ± 0·003					(1)
CeSi	8·306 ± 0·005	3·967 ± 0·003	5·978 ± 0·003					(1)
	8·302 ± 0·002	3·962 ± 0·001	5·964 ± 0·002					(25)
CeGe	8·354 ± 0·005	4·082 ± 0·003	6·033 ± 0·003					(1)
	8·356 ± 0·005	4·084 ± 0·003	6·041 ± 0·004					(26)
PrSi	8·240 ± 0·005	3·941 ± 0·003	5·920 ± 0·003					(1)
	8·29 ± 0·02	3·94 ± 0·01	5·94 ± 0·01					(25)
PrGe [h]	8·288 ± 0·005	4·050 ± 0·003	5·987 ± 0·003					(1)
NdSi	8·156 ± 0·005	3·920 ± 0·003	5·881 ± 0·003					(1)
	8·21 ± 0·02	3·93 ± 0·01	5·89 ± 0·01					(25)
SmSi	8·055 ± 0·005	3·888 ± 0·003	5·804 ± 0·003					(1)
	8·13 ± 0·02	3·90 ± 0·01	5·83 ± 0·01					(25)
GdSi	7·996 ± 0·005	3·859 ± 0·003	5·724 ± 0·003					(1)
	8·00 ± 0·02	3·85 ± 0·01	5·73 ± 0·01					(25)
TbSi	7·919 ± 0·005	3·833 ± 0·003	5·703 ± 0·003					(1)
	7·97 ± 0·02	3·82 ± 0·01	5·69 ± 0·01					(25)
DySi [h]	7·844 ± 0·005	3·820 ± 0·003	5·668 ± 0·003					(1)
	7·87 ± 0·02	3·80 ± 0·01	5·65 ± 0·01					(25)
HoSi [h]	7·808 ± 0·005	3·801 ± 0·003	5·633 ± 0·003					(1)
	7·81 ± 0·02	3·79 ± 0·01	5·63 ± 0·01					(25)
ErSi [h]	7·772 ± 0·005	3·785 ± 0·003	5·599 ± 0·003					(1)
TiB	6·12 ± 0·01	3·06 ± 0·01	4·56 ± 0·01	0·177	0·123	0·029	0·603	(2)
TiSi	$6·54_4$	$3·63_8$	$4·99_7$	0·179	$0·127_5$			(3)
[e]	$6·49_2$	$3·61_8$	$4·97_3$					(4)
TiGe [e]	$6·83_4$	$3·80_8$	$5·23_5$					(4)
ZrSi [b], [c]	$6·98_2$	$3·78_6$	$5·30_1$	0·178	0·125	$0·03_2$	$0·61_1$	(5)
ZrGe [g]	$7·07_5$	$3·90_4$	$5·39_4$					(6)
HfB	6·517	3·218	4·919					(7)
HfSi	$6·85_5$	$3·75_2$	$5·19_1$					(8)
HfGe								(9)
ThSi	7·88	4·15	5·89	0·18	0·13	0·03	0·61	(10)
USi	7·66 ± 0·01	3·91 ± 0·01	5·66 ± 0·01	0·180 ± 0·10	0·125 ± 0·010	0·028	0·611	(11)
PuSi	7·993 ± 0·003	3·847 ± 0·001	5·727 ± 0·005					(12)
MnB	5·560	2·977	4·145	0·180	0·125	0·031	0·614	(13)
FeB	5·506	2·952	4·061	0·180	0·125	0·031	0·620	(14)
CoB	5·254	3·043	3·956	0·180	0·125	0·037	0·625	(15)
Group II compounds								
YNi	7·151 ± 0·001	4·124 ± 0·001	5·513 ± 0·001					(16)
[i]	7·14 ± 0·01	4·114 ± 0·004	5·505 ± 0·008	0·181 ± 0·001	0·132 ± 0·001	0·037 ± 0·001	0·622 ± 0·002	(22)
YPt	7·010 ± 0·001	4·471 ± 0·001	5·552 ± 0·001					(16)
LaCu	7·532	4·625	5·711					(23)
CeCu [f]	7·30 ± 0·02	4·30 ± 0·02	6·36 ± 0·02	0·1670 ± 0·0006	0·1469 ± 0·0007	0·0413 ± 0·0015	0·6034 ± 0·0017	(17)
	7·370	4·623	5·648					(23)
PrPt	7·294 ± 0·001	4·560 ± 0·001	5·698 ± 0·001					(16)
PrCu	7·343	4·584	5·604					(23)
Nd_2NiAu	7·329	4·635	5·728					(23)
NdPt	7·256 ± 0·001	4·551 ± 0·001	5·675 ± 0·001					(16)
NdCu	7·32	4·55	5·59					(23)
SmPt	7·152 ± 0·001	4·525 ± 0·001	5·626 ± 0·001					(16)
SmCu								(27)
GdNi [a], [d]	6·931 ± 0·002	4·353 ± 0·002	5·428 ± 0·002					(18)
Gd_2NiAu	7·153	4·537	5·590					(23)
GdPt	7·088 ± 0·001	4·502 ± 0·001	5·590 ± 0·001					(16)
[a]	7·164 ± 0·003	4·458 ± 0·003	5·574 ± 0·005	0·185	0·144	0·040	0·653	(18)
TbPt	7·018 ± 0·001	4·494 ± 0·001	5·561 ± 0·001					(16)
DyNi	7·043 ± 0·001	4·164 ± 0·001	5·451 ± 0·001					(16)
[a]	6·895 ± 0·002	4·319 ± 0·002	5·353 ± 0·004					(18)
DyPt	6·983 ± 0·001	4·478 ± 0·001	5·544 ± 0·001					(16)
[a]	7·118 ± 0·009	4·453 ± 0·013	5·466 ± 0·011					(18)
HoNi	7·022 ± 0·001	4·140 ± 0·001	5·435 ± 0·001					(16)
[k]	7·016 ± 0·001	4·143 ± 0·001	5·432 ± 0·001					(24)

Table 2 (*cont.*)

	Lattice parameters for setting *Pnma*			Adjustable parameters ($r_A > r_B$)				Ref.
	a(Å)	b(Å)	c(Å)	x_A	z_A	x_B	z_B	
HoPt	6·951 ± 0·001	4·470 ± 0·001	5·532 ± 0·001					(16)
ErNi	6·991 ± 0·001	4·114 ± 0·001	5·418 ± 0·001					(16)
([k])	7·000 ± 0·002	4·118 ± 0·001	5·414 ± 0·001					(24)
ErPt	6·904 ± 0·001	4·453 ± 0·001	5·512 ± 0·001					(16)
TmNi	6·959 ± 0·001	4·099 ± 0·001	5·398 ± 0·001					(16)
([k])	6·960 ± 0·003	4·100 ± 0·002	5·391 ± 0·002					(24)
TmPt	6·855 ± 0·001	4·446 ± 0·001	5·496 ± 0·001					(16)
LuNi	6·912 ± 0·001	4·073 ± 0·001	5·366 ± 0·001	0·185	0·144	0·040	0·653	(16)
([k])	6·910 ± 0·002	4·068 ± 0·002	5·362 ± 0·006					(24)
LuPt	6·810 ± 0·001	4·417 ± 0·001	5·479 ± 0·001					(16)
ThPd	7·249 ± 0·005	4·571 ± 0·003	5·856 ± 0·004	0·180 ± 0·002	0·124 ± 0·002	0·030 ± 0·002$_5$	0·630 ± 0·002$_5$	(19)

([a]) In the original publication, the axes have been interchanged erroneously.
([b]) The a-constant in the cited paper is given correctly in the text, but the value given in the abstract is erroneous.
([c]) A second modification with CrB type was reported by (20).
([d]) A CrB structure type for GdNi is given by (16).
([e]) Ageev & Samsonov (4) reported for TiSi and isotypic TiGe a space group and point positions which do not agree with each other. Principally, their unit cell data are correct, but their structure proposal is erroneous. As TiSi was shown independently by (3) to have the *B*27 structure type, the structure of TiGe obviously must be the same.
([f]) The plot a/b and c/b in Fig. 1 for CeCu, using the lattice parameters of (17), differs rather markedly from all others. Using the CeCu lattice parameters of (23) however, an excellent agreement with the ratios of other compounds is obtained.
([g]) A change in chemical composition from $ZrGe_{1\cdot0}$ to $ZrGa_{0\cdot1}\ Ge_{0\cdot9}$ leads to a structure change from the FeB to CrB structure type (21).
([h]) High temperature modification. The CrB type occurs at lower temperatures.
([i]) From single-crystal photographs the authors of (22) find a monoclinic unit cell with symmetry $P2_1/b$, $\gamma = 90\cdot0 \pm 0\cdot5°$ and parameters $0\cdot245 \pm 0\cdot006$ and $0\cdot249 \pm 0\cdot004$ respectively for Ni and Y instead of the fixed parameters of $\frac{1}{4}$ for a true FeB (*B*27) structure type.
([k]) A second modification with CrB (*B*33) type structure is found by (24).

Table 2 – Literature references

(1) This work.
(2) Decker & Kasper (1954).
(3) Brukl, Nowotny, Schob & Benesovsky (1961)
(4) Ageev & Samsonov (1959).
(5) Schachner, Nowotny & Kudielka (1954).
(6) Schubert, Meissner, Raman & Rossteutscher (1964).
(7) Rudy & Benesovsky (1961).
(8) Nowotny, Laube, Kieffer & Benesovsky (1959).
(9) Nowotny, Benesovsky & Schob (1960).
(10) Jacobsen, Freeman, Tharp & Searcy (1956).
(11) Zachariasen (1949).
(12) Coffinberry & Ellinger (1955).
(13) Kiessling (1950).
(14) Bjurström & Arnfelt (1929).
(15) Bjurström (1933).
(16) Dwight, Conner & Downey (1965*a*).
(17) Larson & Cromer (1961).
(18) Baenziger & Moriarty (1961).
(19) Thomson (1964).
(20) Schob, Nowotny & Benesovsky (1961).
(21) Schubert, Raman & Rossteutscher (1964).
(22) Smith & Hansen (1965).
(23) Dwight, Conner & Downey (1965*b*)
(24) Abrahams *et al.* (1964).
(25) Gladyshevskij & Kripyakevich (1964).
(26) Tharp, Smith & Johnson (1966).
(27) Walline & Wallace (1965)

The occurrence of the FeB (*B*27) structure type

The FeB structure type was first described by Bjurström & Arnfelt (1929) and has received the notation *B*27 in the *Strukturberichte*. Currently some fifty compounds with FeB structure type are known. Unfortunately in some publications the axes have been interchanged erroneously. Table 2 gives a listing of all known compounds with FeB structure type, their lattice constants and positional parameters, corrected wherever necessary for reasons given in the footnotes.

It has been shown in the case of the compounds with CrB structure type (Schob & Parthé, 1965) that these compounds can be separated into different divisions depending on the position of the components in the periodic system. The same has been done in Table 2 for FeB type compounds. The divisions used are similar to those used for CrB type compounds.

Group I *A*. Transition or rare earth metals
B. B, Si, Ge,

Group II *A*. Transition metals of 3rd or 4th group or rare earth metals.
B. Transition metal of 8th group or metal of Cu group.

As before, the *A* component is always bigger than the *B* partner. If the FeB type compounds are plotted in an *a/b versus c/b* diagram shown in Fig. 1, the plots of all compounds are positioned in a narrow band similar as found for CrB type structures (Fig. 1 in the paper by Schob & Parthé, 1965). Group I compounds have their plots in the upper part, group II compounds in the lower part of the band. The same was reported for CrB type structures where group I compounds had their plots in a region different from group II compounds.

Table 3. *Intensity calculation for* HoSi

Cr $K\alpha$ radiation

Low temperature modification ($B33$ or CrB type) $a=4{\cdot}228$, $b=10{\cdot}429$, $c=3{\cdot}801$ Å				High temperature modification ($B27$ or FeB type) $a=7{\cdot}808$, $b=3{\cdot}801$, $c=5{\cdot}633$ Å			
h k l	$10^3 \sin^2\theta_c$	I_c	I_o	*h k l*	$10^3 \sin^2\theta_c$	I_c	I_o
0 2 0	48·2	3·4	—				
				1 0 1	62·9	22·4	*w*
1 1 0	85·5	105·6	*ms*	2 0 0	86·1	48·0	*m*
				2 0 1	127·4	68·5	*m*
				0 1 1	132·2	86·5	*ms*
0 2 1	139·1	177·0	*vs*				
				1 1 1	153·7	175·8	*vvs*
				0 0 2	165·4	1·1	—
1 1 1	176·3	262·9	*vvs*	2 1 0	176·9	131·3	*vvs*
1 3 0	182·0	144·4	*s*				
				1 0 2	186·9	143·4	*vvs*
0 4 0	193·0	74·2	*ms*				
				2 1 1	218·2	71·8	*ms*
				3 0 1	235·0	79·9	*ms*
				2 0 2	251·5	0·0	—
1 3 1	272·8	75·2	*ms*				
				1 1 2	277·7	65·8	*s*
0 4 1	283·8	27·2	*m*				
2 0 0	293·6	57·2	*ms*				
				3 1 1	325·8	7·5	*vvw*
2 2 0	341·9	0·6	—	2 1 2	342·3	0·7	—
				4 0 0	344·4	0·5	—
				3 0 2	359·1	0·8	—
0 0 2	363·3	41·6	*ms*	0 2 0	363·3	41·6	*m*
1 5 0	375·0	1·5	*vw*				
				4 0 1	385·1	30·5	*mw*
				1 0 3	393·7	1·9	—
0 2 2	411·5	0·5	—				
				1 2 1	426·1	3·6	—
2 2 1	432·7	68·3	*s*				
0 6 0	434·3	4·0		4 1 0	435·2	34·4	*m*
1 1 2	448·7	21·2	*mw*	2 2 0	449·4	9·8	*s*
				3 1 2	449·9	64·1	
				2 0 3	458·2	14·0	*w*
1 5 1	465·8	61·7	*s*	0 1 3	463·0	17·9	*w*
				4 1 1	476·5	4·8	—
2 4 0	486·6	39·7	*ms*	1 1 3	484·5	25·0	*w*
				2 2 1	490·7	20·3	*w*
				4 0 2	509·8	0·0	—
0 6 1	525·1	30·8	*m*				
				0 2 2	528·7	0·4	—
1 3 2	545·2	64·7	*s*				
				2 1 3	549·1	29·5	*vs*
				1 2 2	550·2	66·5	
0 4 2	556·3	35·8	*m*				
				3 0 3	565·8	17·4	*vw*
2 4 1	577·4	23·1	*m*	5 0 1	579·4	9·2	*vw*
				3 2 1	598·3	50·4	*s*
				4 1 2	600·6	0·2	—
				2 2 2	614·7	0·0	—
2 0 2	656·9	50·9	*ms*	3 1 3	656·7	2·4	—
				0 0 4	661·6	24·6	*m*
1 7 0	664·5	50·7	*s*				
3 1 0	672·6	8·6	*vw*	5 1 1	670·2	25·0	*m*
				1 0 4	683·1	0·8	—
2 2 2	705·1	0·7	—	5 0 2	703·5	9·4	*vvw*
				4 2 0	707·6	0·5	—
				4 0 3	716·5	29·3	*m*
				3 2 2	722·4	1·0	—
2 6 0	727·9	6·6	*vw*				
1 5 2	738·3	2·1	—				
				2 0 4	747·7	8·8	*s*
				4 2 1	749·0	44·6	
1 7 1	755·3	0·8	—	1 2 3	756·9	3·0	—
3 1 1	763·5	60·6	*s*				

Table 3 (*cont.*)

Low temperature modification ($B33$ or CrB type) $a=4{\cdot}228$, $b=10{\cdot}429$, $c=3{\cdot}801$ Å					High temperature modification ($B27$ or FeB type) $a=7{\cdot}808$, $b=3{\cdot}801$, $c=5{\cdot}633$ Å			
h	k	l	$10^3 \sin^2\theta_c$	I_c	I_o	h k l	$10^3 \sin^2\theta_c$	I_c	I_o
3	3	0	769·2	35·4	*ms*	1 1 4	773·9	1·3	
0	8	0	772·0	6·5		6 0 0	774·8	20·1	*mw*
0	6	2	797·5	7·5	—	5 1 2	794·2	65·6	*s*
						4 1 3	807·3	7·6	—
2	6	1	818·7	73·8	*vs*	6 0 1	816·1	1·5	—
						2 2 3	821·5	29·7	*m*
						2 1 4	838·5	70·9	*s*
2	4	2	849·9	98·0	*vs*				
						3 0 4	855·3	0·0	—
3	3	1	860·0	43·2		0 3 1	858·7	17·6	
0	8	1	862·9	36·2	*vs*				*mw*
0	2	3	865·6	39·4		6 1 0	865·6	18·1	*mw*
						4 2 2	873·0	0·0	—
						1 3 1	880·2	47·2	
1	1	3	902·8	94·8	*vs*	2 3 0	903·5	47·8	
						6 1 1	906·9	45·2	*vs, d*
						5 0 3	910·2	12·9	
						3 2 3	929·1	71·2	*s*
						6 0 2	940·2	0·5	—
						5 2 1	942·7	42·5	*s*
						2 3 1	944·7	47·7	—
						3 1 4	946·1	1·7	
3	5	0	962·2	2·8	—				

Table 4. *Lattice constants of rare earth monosilicides and germanides with* CrB *or* TlI (*B*33) *structure type* (*setting Cmcm*)

Silicides	a(Å)	b(Å)	c(Å)	Reference
EuSi	4·72 ±0·01	11·15 ±0·02	3·99 ±0·01	(2)
DySi	4·237±0·003	10·494±0·005	3·818±0·003	(1)
HoSi	4·228±0·003	10·429±0·005	3·801±0·003	(1)
ErSi	4·197±0·003	10·382±0·005	3·791±0·003	(1)
	4·19 ±0·01	10·40 ±0·02	3·79 ±0·01	(2)
TmSi	4·18 ±0·01	10·35 ±0·02	3·78 ±0·01	(2)
YbSi	4·19 ±0·01	10·35 ±0·02	3·77 ±0·01	(2)
LuSi	4·15 ±0·01	10·24 ±0·02	3·75 ±0·01	(2)
ScSi	3·988±0·002	9·882±0·005	3·659±0·002	(5)
YSi	$4{\cdot}25_1$	$10{\cdot}52_6$	$3{\cdot}82_6$	(6)
	4·257±0·005	10·527±0·008	3·839±0·005	(7)
	4·27	10·53	3·85	(2)
Germanides				
PrGe	4·479±0·003	11·084±0·005	4·050±0·003	(1)
	4·474	11·098	4·064	(3)
NdGe	4·456±0·004	11·027±0·01	4·035±0·004	(8)
	4·442±0·003	11·012±0·005	4·030±0·003	(1)
SmGe	4·36 ±0·01	10·86 ±0·02	4·01 ±0·01	(1)
	4·387±0·004	10·890±0·01	3·993±0·004	(8)
EuGe	4·730±0·004	11·194±0·01	4·105±0·004	(8)
GdGe	4·327±0·003	10·77 ±0·01	3·954±0·003	(1)
	4·339±0·004	10·788±0·01	3·973±0·004	(8)
	4·175±0·002	10·61 ±0·01	3·960±0·003	(4)
TbGe	4·296±0·003	10·709±0·005	3·943±0·003	(1)
	4·300±0·004	10·717±0·01	3·950±0·004	(8)
DyGe	4·263±0·003	10·675±0·01	3·924±0·003	(1)
	4·272±0·004	10·678±0·01	3·931±0·004	(8)
	4·112±0·002	10·81 ±0·02	3·924±0·006	(4)
HoGe	4·234±0·003	10·610±0·005	3·911±0·003	(1)
	4·247±0·005	10·63 ±0·02	3·919±0·005	(8)
ErGe	4·215±0·003	10·567±0·005	3·901±0·003	(1)
	4·20	10·58	3·92	(8)
ScGe	4·007±0·004	10·06 ±0·01	3·762±0·004	(5)
YGe	4·262±0·002	10·694±0·005	3·941±0·002	(5)

(1) This work.
(2) Gladyshevskij & Kripyakevich (1964).
(3) Iandelli (1955).
(4) Baenziger & Moriarty (1961).
(5) Schob & Parthé (1965).
(6) Parthé (1959).
(7) Lundin (1961).
(8) Tharp, Smith & Johnson (1966).

As discussed further below, FeB and CrB type structures have a common structural unit which consists of a row of trigonal prisms of *A* atoms, stacked side on side, centered by a zigzag chain of *B* atoms. The individual trigonal prisms of FeB and CrB type structures have different relative dimensions in group I and group II compounds which lead to the different grouping in the axial ratio diagrams.

A schematic drawing of the different prism shapes for group I and group II compounds is given in Fig. 2. Group I prisms are elongated perpendicular to the zigzag chain direction, while group II prisms are shortened. Since group I prisms are elongated and group II prisms shortened, a prism with a square side (middle drawing of Fig. 2) is a boundary case. One can calculate the possible unit cell axial ratios of FeB structures for such a case. The result is shown graphically in Fig. 1 with a dashed line.

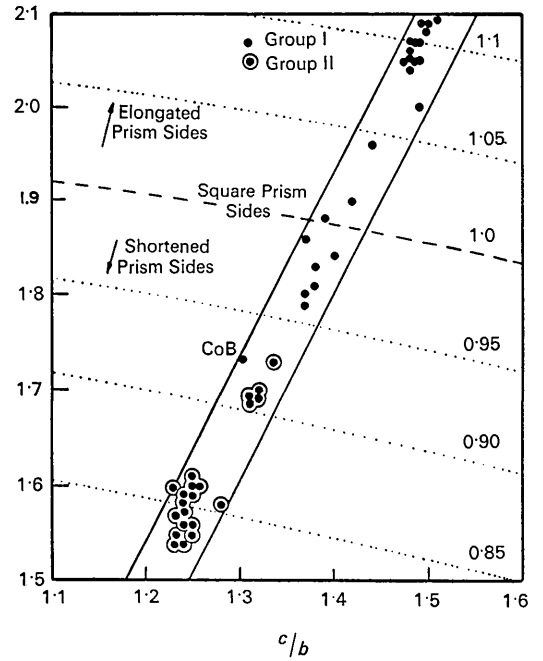

Fig. 1. The axial ratios of the FeB (*B*27) type phases.

In Fig. 1, dotted lines for other shapes of the prism side have also been drawn. The number assigned to each line indicates the ratio for prism length perpendicular to zigzag chain to length parallel to zigzag chain (compare with Fig. 2). Numbers smaller than 1 indicate shortened prisms, numbers bigger than 1, elongated prisms. One sees from the total experimental evidence for FeB structure compounds in Fig. 1 that the actual boundary is slightly shifted from the line for a square side as some of the group I compounds can also have very slightly shortened prisms. Thus, the actual borderline between group I and group II compounds for FeB structures should be drawn for a prism with side ratio of 0·95. The corresponding drawing for CrB type structures (Fig. 1 of Schob & Parthé, 1965) has as abscissa an a_{CrB}/c_{CrB} scale which happens to be also the scale for the side ratio of the prisms in CrB type structures. Also for CrB type structures, the actual borderline between group I and group II compounds should be drawn for a prism side ratio of 0·95.

Compounds with CrB or TlI (*B*33) structure types

The compound HoSi was found to crystallize with two modifications, one of these having the FeB structure type as verified by the intensity calculation shown on the right side of Table 3. The other modification was obtained in slowly cooled samples. The new diffraction pattern could be indexed with an orthorhombic unit cell with:

$$a = 4{\cdot}228 \pm 0{\cdot}003\,, \quad b = 10{\cdot}429 \pm 0{\cdot}005\,,$$
$$c = 3{\cdot}801 \pm 0{\cdot}003\ \text{Å}\,.$$

From the extinctions for *hkl* with $h+k=2n+1$ and *h*0*l* with $l=2n+1$ one finds as possible space groups $Cmc2_1$ (C_{2v}^{12}), $C2cm$ (C_{2v}^{16}) and $Cmcm$ (D_{2h}^{17}). Except for some intensity differences, the pattern of low temperature HoSi is identical to the pattern for YSi which crystallizes with the CrB (*B*33) structure type and has about the same unit-cell dimensions (Parthé, 1959). Taking in account the differences in scattering power between Ho and Y, the differences in the line intensities can be well accounted for. In the left part of Table 3,

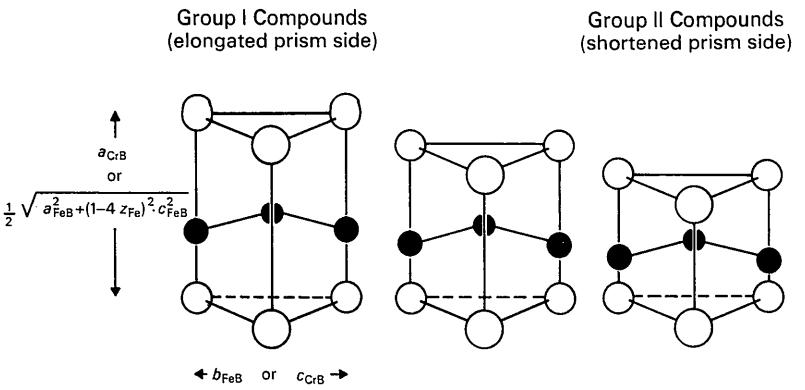

Fig. 2. The different shapes of the trigonal prisms of FeB or CrB type structures in group I and group II compounds.

the intensity values calculated for space group *Cmcm* (D_{2h}^{17}) with 4Ho in 4(*c*) with $y=0{\cdot}141$ and 4Si in 4(*c*) with $y=0{\cdot}426$ and the observed intensity data can be compared. The agreement is good although no efforts were made to sharpen the positional parameters, which are those of PrGe. One can conclude that the low-temperature modification of HoSi crystallizes in the CrB structure type. The calculations for the low-temperature form of HoSi with CrB type structure and the high-temperature form with FeB type structure are arranged in Table 3 with increasing $\sin^2\theta$ values to allow a better observation of the similarity of both patterns.

Two other rare earth silicides (DySi and ErSi), and eight rare earth monogermanides (PrGe, NdGe, SmGe, GdGe, TbGe, DyGe, HoGe and ErGe) were found to be isotypic with the low-temperature form of HoSi (CrB structure type). Their lattice constants are given in Table 4. For completeness, the table contains also earlier data for GdGe and DyGe by Baenziger & Moriarty (1961), PrGe by Iandelli (1955) and the recent data by Gladyshevskii & Kripyakevich (1964) and Tharp, Smith & Johnson (1966).

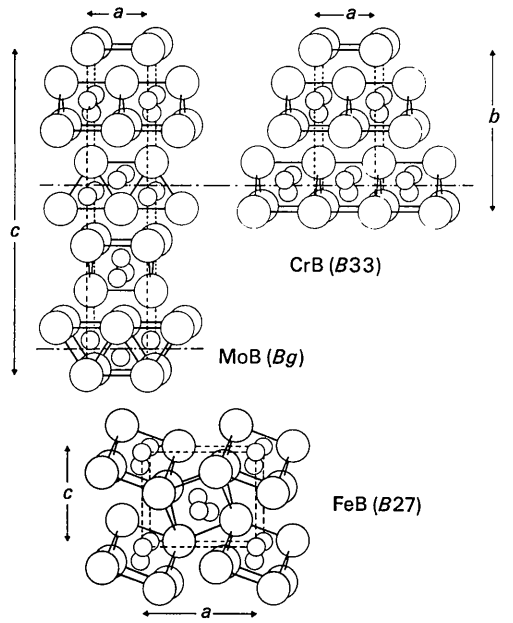

Fig. 3. Perspective drawings of the CrB, MoB and FeB structure types.

The structural relationship between MoB, FeB and CrB structure types

A comparison of Table 2 and Table 4 shows that three rare earth monosilicides and one monogermanide crystallize with both the FeB and the CrB structure type. Experimentally, both structure types have been found in the same arc-melted buttons of these compounds. That part of the button which was in contact with the water cooled copper plate was quenched rapidly; it contained pure FeB type while the slowly cooled part of the button showed the CrB type diffraction lines. It was thus concluded that the FeB type corresponds to a high temperature modification and conversely the CrB type to a low temperature modification.

The common occurrence of both structure types was the cause for a closer look at their structural similarity. Perspective drawings of both types together with the related MoB type are given in Fig. 3. All three structure types are characterized by trigonal prisms which are packed so that they share their rectangular sides in

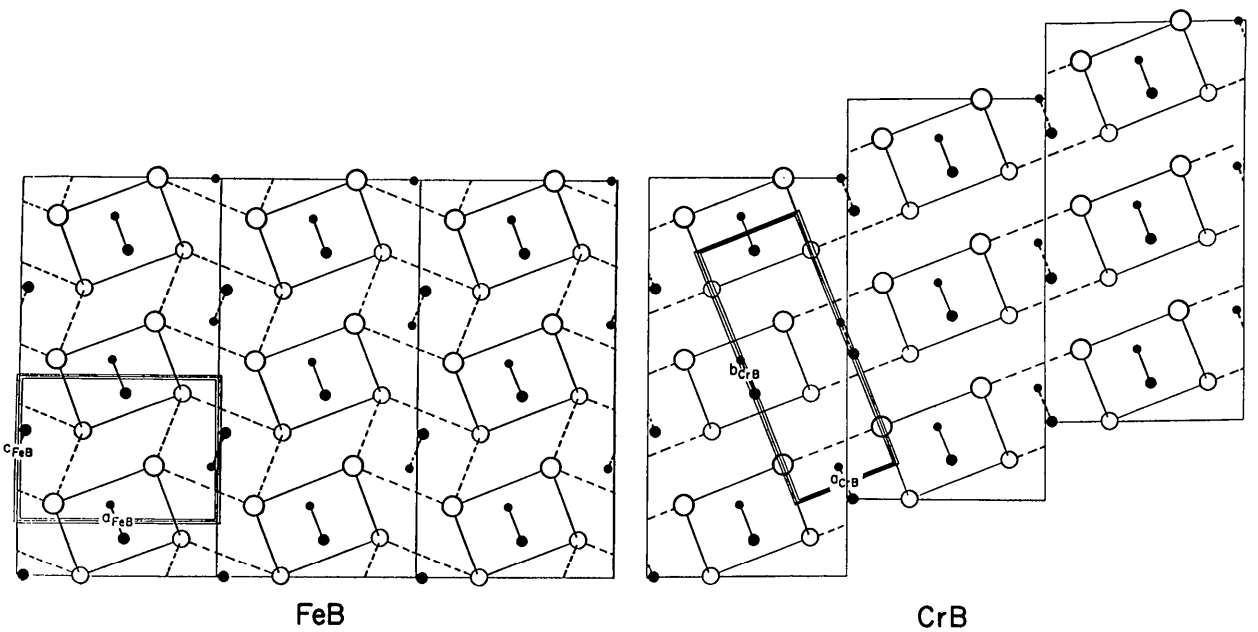

Fig. 4. The geometrical relationships between FeB (*B*27) and CrB (*B*33) structure types.

such a manner that one obtains infinite prism rows which are centered by infinite zigzag chains of the *B* atoms. In the drawing of CrB and FeB the prism rows and thus also the zigzag chains run directly out of the plane of the paper, CrB and FeB structures differing only in the manner these rows are arranged with respect to each other. The tetragonal MoB structure type also contains these rows but some come out of the plane of the paper and some run parallel to the plane of the paper. In the latter case one easily recognizes these chains. The unit cell of the MoB structure is twice as large as the CrB structure cell. One can consider the MoB structure a so-called transposition structure variation of the CrB structure (Boller & Parthé, 1963; Boller, Rieger & Nowotny, 1964). If that half of the MoB structure which is enclosed between the two dash-dot lines is transposed by $\frac{1}{2}\frac{1}{2}0$ (referred to tetragonal axes) one obtains the CrB structure. The side of the prisms in the tetragonal MoB structure must be a square. This condition obviously is not easy to obtain, as only three compounds are known to crystallize with this structure type: MoB, WB and ZrGa. The rare earth silicides and germanides have considerably elongated prisms (prism length ratio of 1·1 in Fig. 1); thus the MoB structure type is not to be expected for these compounds.

No such restrictions for the shape of the trigonal prism exist for FeB and CrB type structures. Also these two structures can be considered as stacking variations, but of a different type*. The left part of Fig. 4 shows a drawing of three blocks each consisting of three unit cells of FeB. If these blocks are shifted in the plane of the paper as seen in the drawing on the right one obtains a structural arrangement as in CrB. The prisms that are not affected by the structural change from FeB to CrB and *vice versa* are drawn with unbroken lines, while broken lines mark the contours of prisms that will be broken up if a change in structure occurs. Thus also the CrB and FeB structure are related to each other like transposition structures, but the magnitude of the transposition vector depends on the values of the positional parameters. For the *idealized case* with $z_B=\frac{5}{8}$ the shift amounts to one half of the *c* translation in FeB.

The unit-cell parameters standing vertically on the plane of the drawing in Fig. 4, *b* in FeB and *c* in CrB, are both determined by the same side of the described trigonal prism (Fig. 2). For a compound crystallizing in both, FeB and CrB structure types (*e.g.* HoSi), considering that the prism dimensions are the same, one can formulate that:

$$b_{\mathrm{FeB}}=c_{\mathrm{CrB}}\,. \qquad (1)$$

That this equation indeed holds quite well can be seen if one compares the observed unit-cell constants for

* We thank Dr Boller for having drawn our attention to this fact.

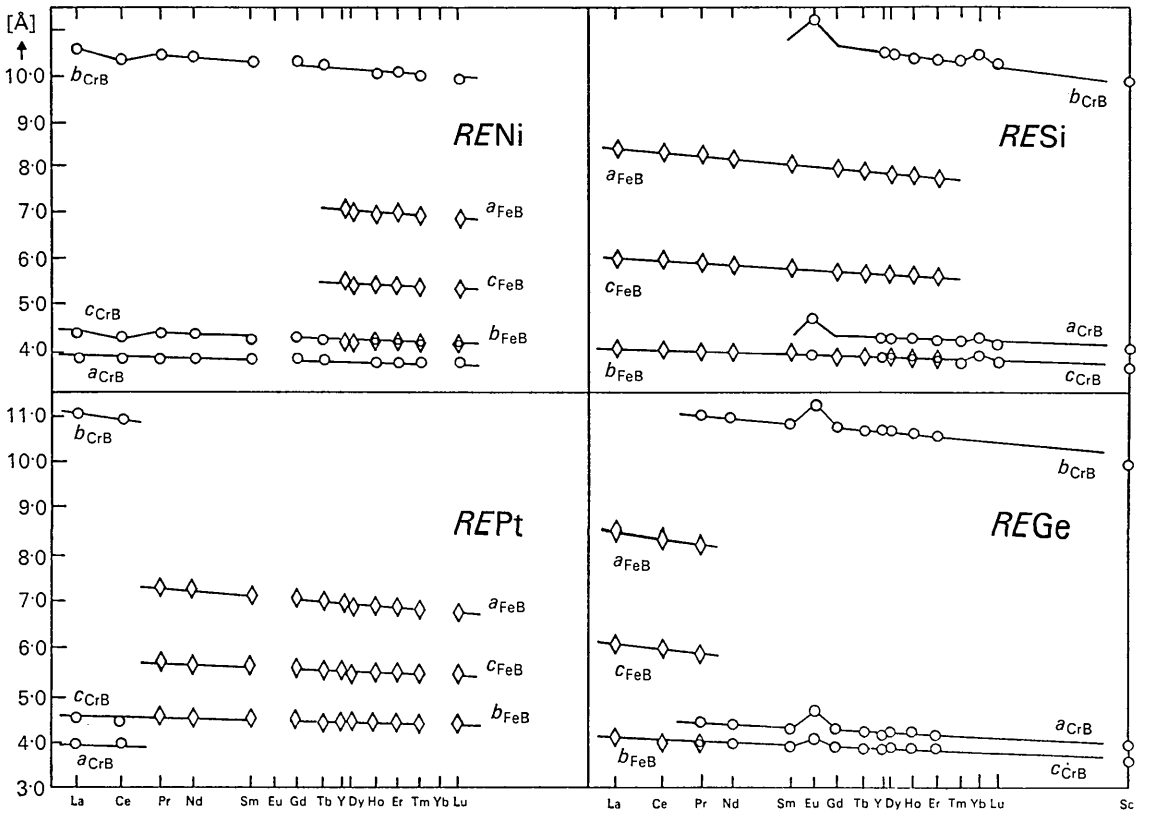

Fig. 5. Unit-cell constants of equiatomic rare earth metal compounds with Si, Ge, Ni, Pt.

HoSi (CrB) and HoSi (FeB) in Table 3 or those of the other compounds exhibiting polymorphism of the same type.

From the geometrical relationship shown in Fig. 4, the equation describing the other base side of the prism can be derived. This equation is seen next to the prism drawing in Fig. 2. It contains a positional parameter, the value of which, unfortunately, is not accurately known for many compounds. For the derivation of the transformation equations, a different, less restricted, geometrical relation is used. That relation can also be deduced from Fig. 4:

$$c_{\mathrm{FeB}}=\tfrac{1}{2}\sqrt{a_{\mathrm{CrB}}^2+b_{\mathrm{CrB}}^2}\,. \qquad (2)$$

In order to complete a set of transformation equations, the final equation can be derived from consideration of the constancy of atomic volume (Rudman, 1965). In excellent agreement with this assumption, the unit-cell volume of CrB type structures is the same as the corresponding FeB cell volume.

$$a_{\mathrm{FeB}}\cdot b_{\mathrm{FeB}}\cdot c_{\mathrm{FeB}}=a_{\mathrm{CrB}}\cdot b_{\mathrm{CrB}}\cdot c_{\mathrm{CrB}}\,. \qquad (3)$$

These equations (1), (2) and (3) are used to derive the following set of transformation equations (4):

$$\begin{aligned} a_{\mathrm{FeB}}&=\frac{2a_{\mathrm{CrB}}\cdot b_{\mathrm{CrB}}}{\sqrt{a_{\mathrm{CrB}}^2+b_{\mathrm{CrB}}^2}}\\ b_{\mathrm{FeB}}&=c_{\mathrm{CrB}}\\ c_{\mathrm{FeB}}&=\tfrac{1}{2}\sqrt{a_{\mathrm{CrB}}^2+b_{\mathrm{CrB}}^2}\,. \end{aligned} \qquad (4)$$

The validity of these equations can be seen in Table 5 where observed and calculated unit cell data of all known compounds with FeB and CrB structure are listed. For silicides and germanides, the agreement is excellent, only for Ni compounds slightly larger deviations are found.

Table 5. *Measured and calculated (equations 4) lattice constants for compounds with* FeB (*B*27) – *structure type**

	a(Å)	*Δ*†	*b*(Å)	*Δ*	*c*(Å)	*Δ*
DySi	7·844	<0·1	3·820	0·0	5·668	0·14
	7·85		3·82		5·66	
HoSi	7·808	0·15	3·801	<0·1	5·633	<0·1
	7·82		3·80		5·63	
ErSi	7·772	<0·1	3·785	0·12	5·599	<0·1
	7·77		3·79		5·60	
PrGe	8·288	<0·1	4·050	0·0	5·987	0·1
	8·29		4·05		5·98	
ZrSi	6·982	0·6	3·782	0·6	5·301	<0·1
	7·02		3·76		5·30	
HoNi	7·016	1·0	4·143	1·5	5·432	0·6
	6·95		4·20		5·40	
ErNi	7·000	0·9	4·118	1·5	5·414	0·4
	6·94		4·18		5·39	
TmNi	6·960	1·0	4·100	1·5	5·391	0·4
	6·89		4·16		5·37	
LuNi	6·910	0·4	4·068	2·5	5·362	0·4
	6·88		4·17		5·34	

* The upper values are observed, the lower values calculated from CrB type data.

† *Δ* is the absolute value of the difference between observed and calculated value of the lattice constants in per cent.

The monosilicides and monogermanides and the other equiatomic rare earth compounds

It was shown earlier in this article that the equiatomic rare earth compounds with Si and Ge crystallize in the FeB and/or CrB structure type. The experimental results are summarized graphically in the right hand part of Fig. 5 including the values for EuGe by Tharp, Smith & Johnson (1966). As ordinate the three unit-cell parameters of each orthorhombic structure were chosen, as abscissa the trivalent ionic rare earth radii r^{3+} as given by Templeton & Dauben (1954). The choice of ionic radii might seem improper as there is probably no, or only a small amount of, ionic bonding in these compounds; however, it is felt that the ionic radii are to be preferred to the metallic radii as the latter ones show a number of irregularities like dips and peaks in the series from La to Lu. The ionic radii instead decrease steadily from La to Lu and they are a true expression for the size of rare earth elements in a particular electronic state. The ionic radii scale can therefore be used as a reference scale if one wants to observe changes in the electronic structure of the rare earth component from one compound to the next.

At the time this study was conducted, three papers were published on other equiatomic rare earth (*RE*) compounds with FeB and CrB structure, the *RE*Ni and *RE*Pt compounds (Dwight, Conner & Downey, 1965*a*; Abrahams, Bernstein, Sherwood, Wernick & Williams, 1964; Walline & Wallace, 1964). It was found useful to compare these results with our results on *RE*Si and *RE*Ge compounds. Diagrams for the unit cell constants of the *RE*Ni and *RE*Pt compounds are given in the left hand part of Fig. 5. For all diagrams shown in Fig. 5, a circle denotes a plot for CrB structure data and a diamond shaped symbol marks data for FeB structures. The sequence of structure types observed first with light rare earth compounds and then with heavy rare earth compounds is reversed for Ni and Pt compounds as compared with Si and Ge compounds. The FeB structure type occurs with heavy *RE*Ni and *RE*Pt compounds but light *RE*Si and *RE*Ge compounds. Conversely the CrB structure is formed with light *RE*Ni and *RE*Pt compounds but heavy *RE*Si and *RE*Ge compounds.

The structural change from CrB to FeB in the case of *RE*Ni compounds and the change from FeB to CrB with *RE*Si compounds occurs late in the series at Ho or Dy. But if the *B* partner is heavier as in *RE*Pt or *RE*Ge compounds the structure change occurs earlier at Pr. Near the transition point some of the compounds may have both structure types concurrently. In this case one can use the transformation equations derived above. One sees clearly that the line for c_{CrB} leads directly into the line for b_{FeB}. The elementary prism in *RE*Ni and *RE*Pt compounds is shortened, but in *RE*Si

and *RE*Ge compounds elongated. Therefore in the left hand diagrams the line for a_{CrB} is below the line for c_{CrB}, but in the right hand diagrams above the line for c_{CrB}.

The data for EuSi and to a lesser degree for YbSi deviate from the straight lines formed by connecting data points for other rare earth compounds. In addition EuSi crystallizes with the CrB structure type although both its neighbour compounds have the FeB structure type. The electronic structure of these two elements in their compounds is different from those of their neighbour atoms in the corresponding compounds resulting in larger size of the atoms. The side ratio of the prism of EuSi with 1·18 falls in the same group as that of the alkaline earth silicides CaSi and SrSi.

At the present it is not possible to predict the occurrence of FeB- or CrB-type structures from bonding considerations. However, if one plots the crystal structure type of all equiatomic compounds *AB versus* the valence electron concentration (VEC), where *A* is an element of the alkaline earth, rare earth or titanium group and *B* an element of the Ni, Cu, Zn, Ga, Ge, As or Se group, one observes:

NaCl ($B1$) type structures for ..... $4 \leq \mathrm{VEC} \leq 4{\cdot}5$,

CrB ($B33$), MoB (B_g) or FeB ($B27$) type structures (group I, elongated prism base) for..... $3 \leq \mathrm{VEC} \leq 4$,

CsCl ($B2$) type structures for ..... $2 \leq \mathrm{VEC} \leq 3$,

CrB ($B33$) or FeB ($B27$) type structures (group II, shortened prism base) for ..... $1{\cdot}5 \leq \mathrm{VEC} \leq 2$. (Assuming Ni-group elements have no valency electrons).

Within CrB, FeB and MoB type structures of group I the prism side ratio varies with the difference of valence electrons Δ between components *A* and *B*. For alkaline earth silicides, germanides or stannides ($\Delta = 2$) the prism side ratio is $\sim 1{\cdot}18$; for rare earth silicides and germanides ($\Delta = 1$), except Eu compounds, a side ratio of $\sim 1{\cdot}10$ is observed. Compounds with $\Delta = 0$ like TiSi, ZrSi or the rare earth gallides have side ratios of the prism below 1·06.

This study is a contribution of the Laboratory for Research on the Structure of Matter, University of Pennsylvania, supported by the Advanced Research Projects Agency, Office of the Secretary of Defense.

References

ABRAHAMS, S. C., BERNSTEIN, J. L., SHERWOOD, R. C., WERNICK, J. H. & WILLIAMS, H. J. (1964). *J. Phys. Chem. Solids* **25**, 1069.

AGEEV, N. V. & SAMSONOV, V. (1959). *Russ. J. Inorg. Chem.* **4**, 716.

BAENZIGER, N. C. & MORIARTY, J. L., JR. (1961). *Acta Cryst.* **14**, 946.

BJURSTRÖM, T. & ARNFELT, H. (1929). *Z. Phys. Chem.* **B4**, 469.

BJURSTRÖM, T. (1933). *Ark. Kemi, Min. Geol.* **11A**, 12.

BOLLER, H. & PARTHÉ, E. (1963). *Acta Cryst.* **16**, 1095.

BOLLER, R., RIEGER, W. & NOWOTNY, H. (1964). *Mh. Chem.* **95**, 1497.

BRUKL, C., NOWOTNY, H., SCHOB, O. & BENESOVSKY, F., (1961). *Mh. Chem.* **92**, 781.

BUERGER, M. J. (1960). *Crystal Structure Analysis*, p. 231. New York: John Wiley.

COFFINBERRY, A. S. & ELLINGER, F. H. (1955). U.S.A. rep. A/Conf. 8/P/826. Abstracted in PEARSON, W. B. (1958), *A Handbook of Lattice Spacings and Structures of Metals and Alloys*. New York: Pergamon Press.

DECKER, B. F. & KASPER, J. S. (1954). *Acta Cryst.* **7**, 77.

DWIGHT, A. E., CONNER, R. A., JR. & DOWNEY, J. W. (1965*a*). *Acta Cryst.* **18**, 835.

DWIGHT, A. E., CONNER, R. A., JR. & DOWNEY, J. W. (1965*b*). Paper presented at Fifth Rare Earth Research Conference, Ames, Iowa.

GLADYSHEVSKII, E. I. & KRIPYAKEVICH, P. I. (1964). *Zh. Strukturnoi Khim.* **5**, 853.

IANDELLI, A. (1955). *Rend. Accad. Lincei*, **19**, 307.

JACOBSON, E. L., FREEMAN, R. D., THARP, A. G. & SEARCY, A. W. (1956). *J. Amer. Chem. Soc.* **78**, 4850.

KIESSLING, R. (1950). *Acta Chem. Scand.* **4**, 146.

LARSON, A. C. & CROMER, D. T. (1961). *Acta Cryst.* **14**, 545.

LUNDIN, C. E. (1961). In *Rare Earth Research*, ed. E. V. Kleber, p. 306. New York: Macmillan.

MOORE, F. H. (1963). *Acta Cryst.* **16**, 1169.

NOWOTNY, H., LAUBE, E., KIEFFER, R. & BENESOVSKY, F. (1958). *Mh. Chem.* **89**, 701.

PARTHÉ, E. (1959). *Acta Cryst.* **12**, 559.

PARTHÉ, E., HOHNKE, D., JEITSCHKO, W. & SCHOB, O. (1965). *Naturwissenschaften* **52**, 155.

RUDMAN, P. S. (1965). *Trans. Met. Soc. AIME*, **233**, 864.

RUDY, E. & BENESOVSKY, F. (1961). *Mh. Chem.* **92**, 415.

SCHACHNER, H., NOWOTNY, H. & KUDIELKA, H. (1954). *Mh. Chem.* **85**, 11.

SCHOB, O., NOWOTNY, H. & BENESOVSKY, F. (1961). *Mh. Chem.* **92**, 1218.

SCHOB, O., & PARTHÉ, E. (1964). *Mh. Chem.* **95**, 1466.

SCHOB, O. & PARTHÉ, E. (1965). *Acta Cryst.* **19**, 214.

SCHUBERT, K., MEISSNER, H. G., RAMAN, A. D. & ROSSTEUTSCHER, W. (1964). *Naturwissenschaften*, **51**, 287.

SCHUBERT, K., RAMAN, A. & ROSSTEUTSCHER, W. (1964). *Naturwissenschaften*, **51**, 506.

SMITH, J. F. & HANSEN, D. A. (1965). *Acta Cryst.* **18**, 60.

TEMPLETON, D. H. & DAUBEN, C. H. (1954). *J. Amer. Chem. Soc.* **76**, 5237.

THARP, A. G., SMITH, G. S. & JOHNSON, Q. (1966). *Acta Cryst.* **20**, 583.

THOMSON, J. R. (1964). *Acta Cryst.* **17**, 64.

WALLINE, R. E. & WALLACE, W. E. (1964). *J. Chem. Phys.* **41**, 1587.

WALLINE, R. E. & WALLACE, W. E. (1965) *J. Chem. Phys.* **42**, 604.

ZACHARIASEN, W. H. (1949). *Acta Cryst.* **2**, 94.